

IMAGES IN NUCLEAR CARDIOLOGY

Cardiac Sarcoidosis Mimicking Anterior Myocardial Infarction

Kyoko Oyama-Suzuki, MD¹⁾, Kenji Fukushima, MD, PhD^{1),2)}, Ryuta Egi, MD¹⁾,
Shintaro Nakano, MD, PhD¹⁾ and Toshihiro Muramatsu, MD, PhD¹⁾

Received: October 27, 2020/Revised manuscript received: March 23, 2021/Accepted: April 12, 2021

J-STAGE advance published: June 15, 2021

© The Japanese Society of Nuclear Cardiology 2021

Abstract

A 58-year-old asymptomatic man with electrocardiogram (ECG) abnormality was referred to our institution for cardiac exams. His ECG showed a bifascicular block, and the echocardiography demonstrated a wall motion abnormality in apex. Stress-rest myocardial perfusion imaging (MPI) showed a significant defect in anterior wall with partial redistribution at rest. He was suspected of having an anterior myocardial infarction (MI) and underwent cardiac catheterization. However, coronary angiography (CAG) revealed no significant coronary atherosclerosis. Cardiovascular magnetic resonance imaging (CMR) was performed to evaluate the extent of myocardial infarction. Late gadolinium enhancement (LGE) demonstrated a significant epicardial and mid-myocardial LGE in the multiple site including anterior, anteroseptal, lateral, inferior wall, and basal right ventricle junction, which strongly indicated that the fibrosis was due to cardiac sarcoidosis (CS). A myocardial perfusion defect in anterior wall shown in the MPI revealed the fibrosis as an atypical finding mimicking anterior MI.

Keywords: Cardiac Magnetic Resonance Imaging, Cardiac sarcoidosis, Cardiomyopathy, Myocardial perfusion imaging

Ann Nucl Cardiol 2021; 7 (1): 73–76

Cardiac sarcoidosis (CS) is cardiac manifestation of a multisystem granulomatous inflammatory disease of unknown etiology, and causes lethal arrhythmias, heart failure, and sudden death. However, the diagnosis of CS is still challenging due to the low sensitivity of endomyocardial biopsy (EMB) (1). Therefore, clinical diagnosis using cardiac magnetic resonance imaging (CMR), positron emission tomography (PET), and myocardial perfusion imaging (MPI) are known to be useful strategies. These imaging modalities are included in criteria for clinical diagnosis of CS. CS is known to show focal fibrosis predominantly in the basal anteroseptal wall. In the present case, we experienced the patient who was clinically diagnosed of CS by CMR, despite of showing significant anterior defect in MPI and normal coronary artery. This patient showed an anterior defect in the MPI, which was suggestive of infarction, while coronary angiography (CAG) revealed a normal coronary. However, the CMR showed a typical late gadolinium enhancement (LGE)

pattern compatible with CS, and the MPI findings were indistinguishable from anterior myocardial infarction (MI).

Case report

A 58-year-old man with history of hyperuricemia and alcohol-related liver dysfunction was referred to our institution. A screening electrocardiogram (ECG) showed bifascicular block. He underwent further cardiac tests, and an echocardiography demonstrated a slight wall thickening in left ventricular septum without wall motion abnormality. We followed up on the patient's progress for a year, and a follow up echocardiography detected an anterior wall motion abnormality. He underwent a stress-rest ²⁰¹Tl MPI study, and the MPI showed a significant anterior defect and partial tracer redistribution at rest which strongly suggested myocardial infarction with obstructive diagonal branch of the left anterior descending artery. The ECG gated MPI showed a significant

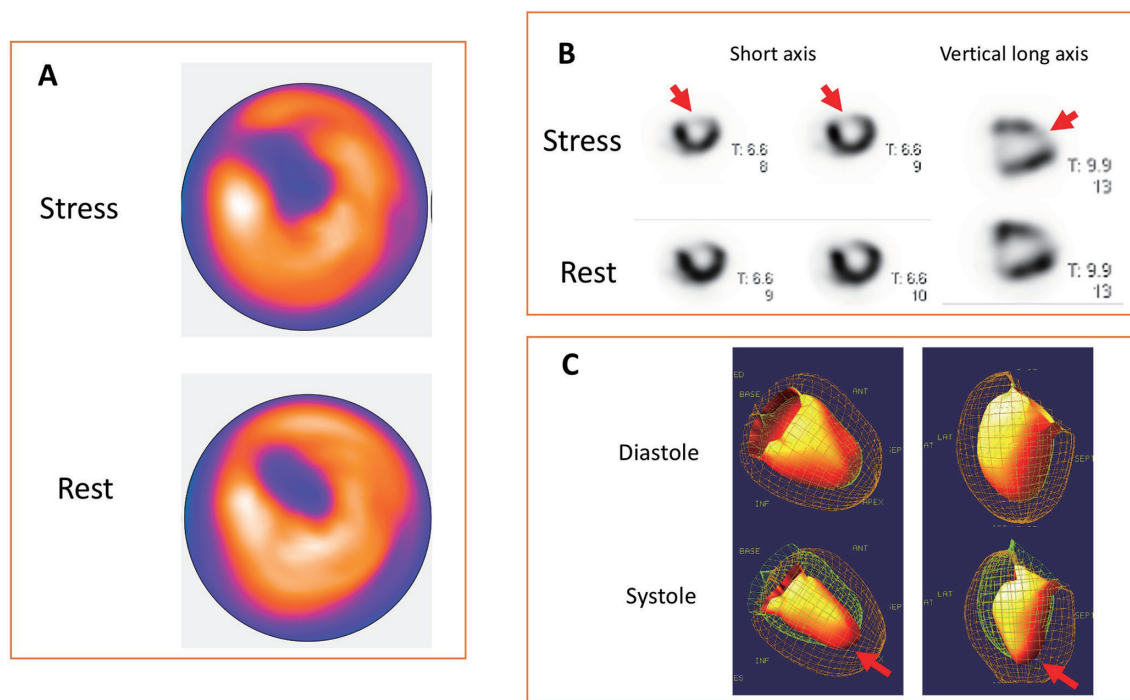


Figure 1 ECG gated ^{201}Tl stress-rest MPI were shown. The MPI showed significant anterior defect and partial redistribution which strongly indicated myocardial infarction in the territory of diagonal branch or distal site of left anterior descending artery. A polar map output is shown in A, and short and transvers axis views are shown in B (upper and lower for stress and rest; defect was pointed by red arrows). ECG gated SPECT images which demonstrated significant dyskinesia in anterior wall (C, red arrows).

wall motion abnormality in the anterior wall which was consistent with anterior infarction (Figure 1). He underwent a CAG following positive MPI. However, CAG showed no obstructive coronary artery, and left ventriculography (LVG) showed significantly reduced systolic function with an aneurysm in the basal anterior wall (LVEF 35%) (Figure 2 upper). He underwent CMR to evaluate the aneurysm and the extent of the anterior infarction. Cine-CMR demonstrated significantly regional myocardial thinning in the basal anterior wall. However, LGE showed a significant epicardial to transmural pattern in multiple sites such as anteroseptal to lateral, and inferior wall which strongly indicated CS. A sagittal two chamber view of LGE image showed that the fibrosis expanded to the apical wall which corresponded to perfusion defect in the MPI (Figure 2 lower). The patient was clinically diagnosed with CS because he met the diagnostic criteria (LGE in CMR, regional wall thinning in the basal area, and the anterior wall aneurysm as major criteria; an abnormal ECG finding, and the perfusion defect in the MPI as minor criteria).

Discussion

In this case report, we encountered the case with significant anterior perfusion defect despite normal coronary, and CMR revealed epicardial LGE which was strongly suspect of CS. The diagnosis of CS is still challenging despite of advances in

imaging techniques and serum biomarkers (2). A definite diagnosis should be based on histological examination by EMB. However, EMB has limited sensitivity, and the clinical diagnosis based on the guidelines is widely performed (3). Recent technical advances in noninvasive imaging has thoroughly explained the low sensitivity of EMB due to the focal nature of the disease in the myocardium. Clinical manifestations of CS, such as conduction abnormalities, fatal arrhythmias, and heart failure, are relatively non-specific findings. Thus, clinical diagnosis using non-invasive imaging based on the guidelines were frequently performed in clinical practice (3). The accumulated evidence showed the distinctive LGE pattern of CS is from the epicardial to the intramural layers with focal or diffuse-patchy distribution. Additionally, LGE most commonly appears in the basal area of the anterior and anteroseptal wall (4). In the early studies of CS, Yamagishi et al. reported that the myocardial perfusion defect is predominantly located in basal site of anterior and anteroseptal wall (5). In this case, the perfusion defect for the MPI was observed in the mid-anterior wall to apex which seemed to be quite an atypical finding mimicking anterior myocardial infarction. LVG showed significant left ventricular regional aneurysm, while no obstructive coronary stenosis was observed. CMR revealed typical LGE distribution indicating CS. In cine-CMR, anterobasal thinning which can be physiological wall thinning, but LGE was expand to

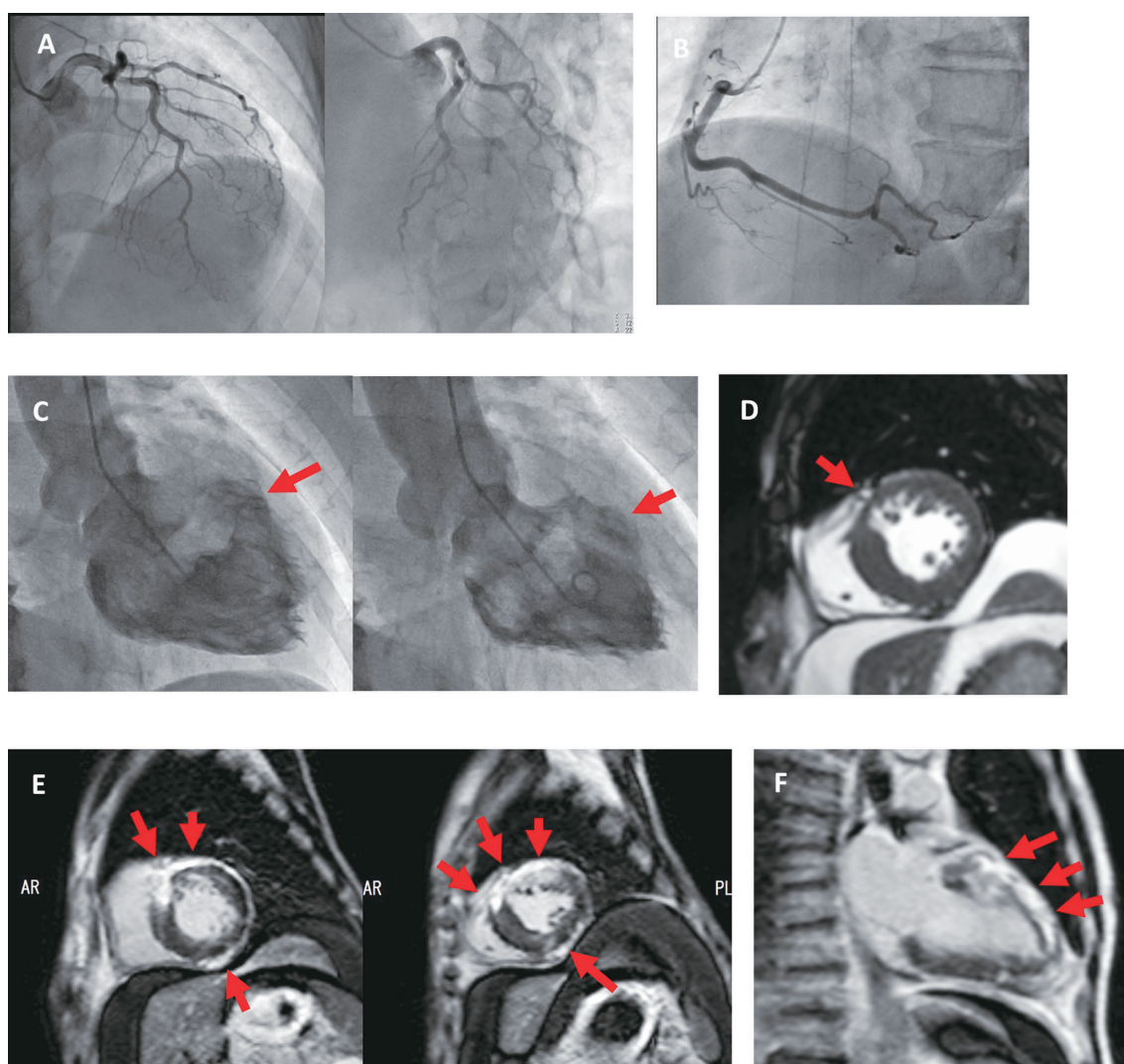


Figure 2 Coronary angiography showed no evidence of coronary artery stenosis (A: showed left coronary artery, and B showed right coronary artery). Left ventriculography showed reduced global systolic function (LVEF 35%), and significant regional aneurysm in mid anterior wall was observed (C, red arrow). The lower displayed cardiac magnetic resonance (CMR) images. Cine-CMR showed significant regional wall thinning in antero-septal wall (D). Late enhancement study demonstrated significant subepicardial to transmural distribution of late gadolinium enhancement (LGE) in antero-septal to lateral, and inferior wall (E, red arrows). Longitudinal two-chamber views showed the LGE has expanded to mid-anterior to apical wall (F, red arrows).

anterobasal area. The insignificant perfusion defect in basal site might be due to non-transmural magnitude of fibrosis and low spatial resolution TL images. Cine-CMR showed anterior aneurysm and relatively thickened septal wall which is frequently observed as typical CS (3). In this case, the partial redistribution in anterior wall was observed. It is speculated that there might be microvascular complications due to the transition from the active inflammation to the irreversible scar. The expanding fibrosis can injure microvascular network, and lead the transient myocardial perfusion defect. MPI is usually employed to detect myocardial ischemia due to obstructive coronary artery disease, while CMR mostly plays main role to explore the etiology of reduced cardiac function or regional wall motion. In this case, the need for differential diagnosis for unexplained anterior defect with normal coronary drove the

patient to CMR study. Consideration for other diagnostic modalities is crucial to elucidate the discrepancy of the MPI and CAG in the assessment of coronary artery disease.

These are several limitations of this report that should be noticed. Clinical diagnosis was done without ^{18}F -fluorodeoxyglucose positron emission tomography. EMB was not performed due to the routine clinical course of assessing coronary artery disease. The discrepancy was observed between ECG gated MPI and LVG due to the insufficient spatial resolution. However, LGE pattern and regional aneurysm were consistent of CS rather than other non-ischemic cardiomyopathy such as hypertrophic cardiomyopathy, amyloidosis, post myocarditis. Nevertheless, in the diagnostic process of coronary artery disease, the need for the evaluation by the multimodality imaging technique is

recommended when the patient shows discrepancies in the findings between MPI and CAG.

Acknowledgments

None.

Sources of funding

None.

Conflicts of interest

The authors declare no conflict of interest.

Reprint requests and correspondence:

Kenji Fukushima, MD, PhD
Department of Nuclear Medicine, Saitama Medical University International Medical Center, 1397-1 Yamane, Hidaka City, Saitama, 350-1298 Japan
E-mail: kfukush4@saitama-med.ac.jp

References

1. Graziosi M, Nanni C, Lorenzini M, Diemberger I, Bonfiglioli R, Pasquale F, et al. Role of ^{18}F -FDG PET/CT in the diagnosis of infective endocarditis in patients with an implanted cardiac device: a prospective study. *Eur J Nucl Med Mol Imaging* 2014; 41: 1617–23.
2. Birnie DH, Nery PB, Ha AC, Beanlands RS. Cardiac sarcoidosis. *J Am Coll Cardiol* 2016; 68: 411–21.
3. Terasaki F, Azuma A, Anzai T, Ishizaka N, Ishida Y, Isobe M, et al. JCS 2016 guideline on diagnosis and treatment of cardiac sarcoidosis–Digest version. *Circ J* 2019; 83: 2329–88.
4. Hulten E, Aslam S, Osborne M, Abbasi S, Bittencourt MS, Blankstein R: Cardiac sarcoidosis–state of the art review. *Cardiovasc Diagn Ther* 2016; 6: 50–63.
5. Yamagishi H, Shirai N, Takagi M, Yoshiyama M, Akioka K, Takeuchi K, et al. Identification of cardiac sarcoidosis with ^{13}N - NH_3 / ^{18}F -FDG PET. *J Nucl Med* 2003; 44: 1030–6.